Louisiana State University
LSU Digital Commons

Faculty Publications | Department of Physics & Astronomy

5-28-2009

# Neutron capture on $^{130}$Sn during r-process freeze-out

J. Beun
*NC State University*

J. C. Blackmon
*Louisiana State University*

W. R. Hix
*Oak Ridge National Laboratory*

G. C. McLaughlin
*NC State University*

M. S. Smith
*Oak Ridge National Laboratory*

*See next page for additional authors*

Follow this and additional works at: https://digitalcommons.lsu.edu/physics_astronomy_pubs

## Recommended Citation

Beun, J., Blackmon, J., Hix, W., McLaughlin, G., Smith, M., & Surman, R. (2009). Neutron capture on $^{130}$Sn during r-process freeze-out. *Journal of Physics G: Nuclear and Particle Physics, 36* (2) https://doi.org/10.1088/0954-3899/36/2/025201

This Article is brought to you for free and open access by the Department of Physics & Astronomy at LSU Digital Commons. It has been accepted for inclusion in Faculty Publications by an authorized administrator of LSU Digital Commons. For more information, please contact ir@lsu.edu.

Authors
J. Beun, J. C. Blackmon, W. R. Hix, G. C. McLaughlin, M. S. Smith, and R. Surman

This article is available at LSU Digital Commons: https://digitalcommons.lsu.edu/physics_astronomy_pubs/283

arXiv:0806.3895v1 [nucl-th] 24 Jun 2008

# Neutron capture on $^{130}$Sn during $r$-process freeze-out

**J. Beun[1], J. C. Blackmon[2], W. R. Hix[3], G. C. McLaughlin[1], M. S. Smith[3], R. Surman[4]**

[1] Department of Physics, North Carolina State University, Raleigh, NC 27695-8202
[2] Department of Physics, Louisiana State University, Baton Rouge, LA 70803
[3] Physics Division, Oak Ridge National Laboratory, Oak Ridge, TN 37831-6374
[4] Department of Physics, Union College, Schenectady, NY 12308

E-mail: jbbeun@ncsu.edu

**Abstract.** We examine the role of neutron capture on $^{130}$Sn during $r$-process freeze-out in the neutrino-driven wind environment of the core-collapse supernova. We find that the global $r$-process abundance pattern is sensitive to the magnitude of the neutron capture cross section of $^{130}$Sn. The changes to the abundance pattern include not only a relative decrease in the abundance of $^{130}$Sn and an increase in the abundance of $^{131}$Sn, but also a shift in the distribution of material in the rare earth and third peak regions.

## 1. Introduction

Experiments at the Holifield Radioactive Ion Beam Facility (HRIBF) at Oak Ridge National Laboratory (ORNL) are currently underway to acquire the nuclear data necessary to help generate precision neutron capture cross sections for neutron-rich nuclei near the $N = 82$ closed shell. This data is relevant to the astrophysical community, since the nucleosynthetic origin of most of the nuclei heavier than the Fe group ($Z \gtrsim 26$) arises from processes involving neutron capture. In particular, the neutron capture rates for the $N = 82$ closed shell operate during the rapid neutron capture process, known as the $r$-process [1, 2].

The classical $r$-process proceeds primarily through two phases, first, an equilibrium phase marked by $(n, \gamma) \rightleftharpoons (\gamma, n)$ equilibrium, and then a freeze-out phase marked by the interplay between neutron capture and photo-dissociation. Early in the $r$-process, both neutron capture and photo-disintegration are fast, hence $(n, \gamma) \rightleftharpoons (\gamma, n)$ equilibrium is established, and the abundance of the nuclear species along each isotopic chain can be found through the Saha equation, for a review see Cowan et al. 1991 [3]. At late times in the $r$-process, $(n, \gamma) \rightleftharpoons (\gamma, n)$ equilibrium fails as the abundance of free neutrons is depleted and the neutron-to-seed ratio of the $r$-process falls below one, $R \lesssim 1$. During this freeze-out epoch of the $r$-process, individual neutron capture and photo-disintegration reactions now play a role in determining the final $r$-process abundance pattern.

The relevant nuclear data for many of the large number of nuclei ($\gtrsim 3000$) which participate in the $r$-process is sparse, see *e*.g. Pearson et al. 2006 [4]. This is particularly true for the neutron capture cross sections. Calculations of the $r$-process employ primarily phenomenological models of neutron capture cross sections that use theoretical nuclear mass models as inputs. The neutron capture cross section of a single nucleus can vary by several orders of magnitude between individual theoretical models, and an example of this is shown in figure 1 for three sets of theoretical neutron capture cross sections based on the SMOKER model [3], the FRDM model [5], and the ETFSI model [6]. To date there has been little calibration with experiment.

Proposed environments for the $r$-process include the neutrino-driven wind of a core-collapse supernova [7, 8, 9, 10, 11, 12, 13, 14, 15, 16, 17], a prompt explosion from a low mass supernova [18, 19], compact object mergers [20, 21, 22], a gamma ray burst accretion disk [23, 24, 25], a collapsar from a massive stellar progenitor [26, 27], and the shocked surface layers of the post-collapse O-Ne-Mg Cores [28, 29]. No single site containing all of the essential ingredients for the $r$-process has been fully realized, however. As such, many recent studies of the $r$-process have focused on understanding how an $r$-process would obtain given the current understanding of the astrophysical conditions. Although the freeze-out epoch of the $r$-process presents a smaller contribution to the final $r$-process abundance pattern than that of the $(n, \gamma) \rightleftharpoons (\gamma, n)$ equilibrium epoch, knowledge of the details of the dynamics of $r$-process freeze-out will be necessary for understanding the fine structure of the abundance

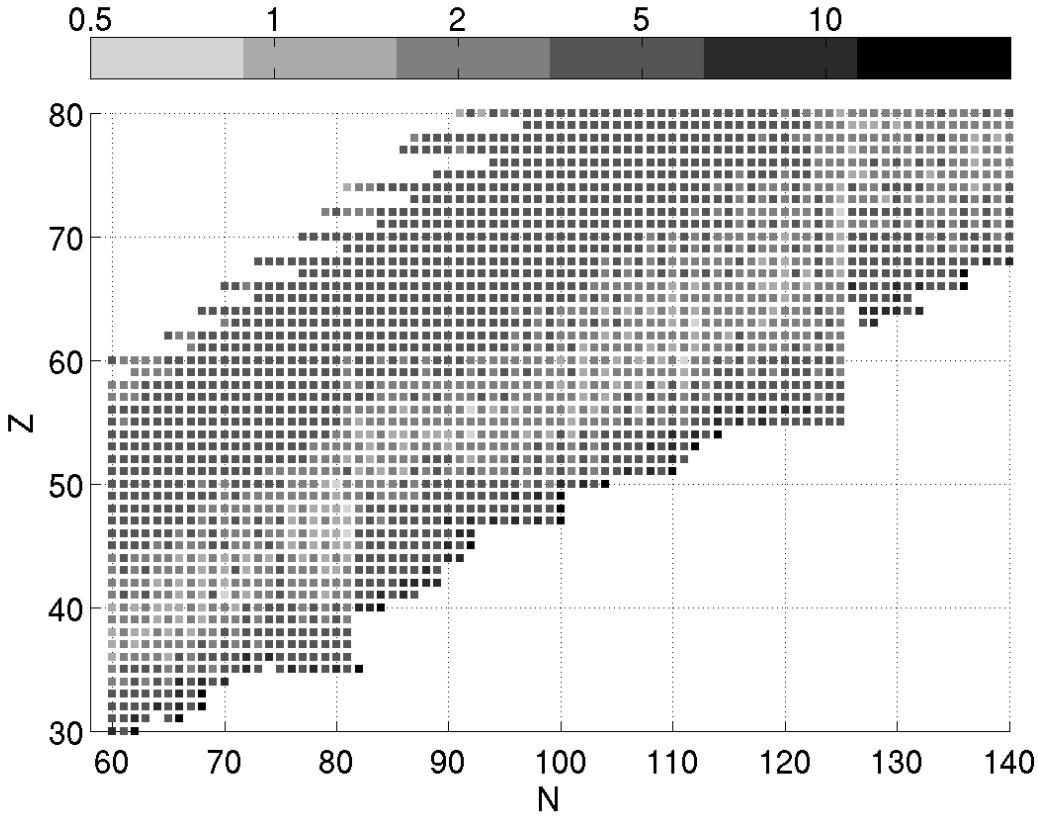


**Figure 1.** We show the ratio (logarithmic) of the largest neutron capture cross section with respect to the smallest neutron capture cross section between three sets of theoretical neutron capture cross sections. The neutron capture cross sections can vary by many orders of magnitude between the theoretical models (ratios $\gtrsim 10^{10}$ for the darkest squares).

pattern as a clearer picture of the astrophysical environment of the $r$-process begins to emerge.

Previous works that have examined the role of neutron capture cross sections in the $r$-process follow two main strategies. Surman and Engel 2001 [30] showed that individual neutron capture cross sections in the region of $A \sim 195$ can influence the $r$-process in this same region during freeze-out. Other works have examined global changes to the cross sections [31, 32, 33, 34, 35], and, in particular, Rauscher 2005 [31] examined how simultaneously changing all the $r$-process neutron capture cross sections can influence the time at which $r$-process freeze-out begins.

We explore how an increase to the neutron capture cross section of $^{130}$Sn can yield global changes to the abundance pattern of the $r$-process compared to an $r$-process calculation under the original, unaltered neutron capture cross sections. Experiments at HRIBF are in progress to collect data for $^{130}$Sn for the first time [36]. We organize this paper as follows. In section 2, we describe the details of our $r$-process calculation

in the neutrino-driven wind. Section 3 describes the factors that enable $^{130}$Sn to become influential to the $r$-process and the physics of the changes to the abundance pattern incurred by increasing the $^{130}$Sn neutron capture cross section. Additionally, in this section we contrast our results for $^{130}$Sn with another nucleus under experimental examination, $^{132}$Sn [37]. We conclude in section 4.

## 2. Model of $r$-process Nucleosynthesis

Using the conditions of the neutrino-driven wind of the core-collapse supernova environment as our guide, we track the evolution of a mass element from the surface of the protoneutron star in order to examine the effects of individual neutron capture cross sections at late times in the $r$-process. We employ a 1D thermodynamic model of the neutrino driven wind as described in [38, 39]. We choose a set of wind conditions that yield the production of $r$-process elements through the third peak. Unless stated otherwise, our calculations employ an entropy per baryon of $s/k = 100$, an outflow timescale of $\tau = 0.3$ s, and an initial electron fraction of $Y_e = 0.26$ at $T_9 = 10$.

To model the nucleosynthesis outcome, we employ two coupled reaction networks to track the abundance of the ejected mass element. While the mass element is near the surface of the proto-neutron star, $T_9 \lesssim 10$, we employ an intermediate network calculation [40] that includes the strong and electromagnetic rates found in [41]. Once material reaches the $r$-process epoch, $T_9 \approx 2.5$, we transition to an $r$-process network [42, 43] that includes the relevant reactions of $\beta$-decay, $\beta$-delayed neutron emission, neutron capture, and photo-disintegration. We use $\beta$-decay rates from [44], neutron separations from [45], and neutron capture rates from [41]. Additional details of the network calculation can be found in [38]. In this initial study, as the changes to the $r$-process pattern occur late in the nucleosynthesis epoch, we do not include neutrino interactions other than to set the initial electron fraction. The $r$-process abundance pattern produced under these conditions in the neutrino-driven wind is shown in figure 2.

## 3. $^{130}$Sn (n,$\gamma$) at Late Times

Near the end of $r$-process freeze-out, while the free neutron abundance is rapidly falling, but neutron capture continues to be a relevant reaction in the $r$-process, $^{130}$Sn becomes highly populated as material flows along the $A = 130$ $\beta$-decay reaction pathway. This pathway is significant as $^{130}$Cd is a closed shell nucleus which is highly populated and has a short $\beta$-decay lifetime, along with its daughter nucleus $^{130}$In. The fraction of material that the now highly populated $^{130}$Sn directs along the $Z = 50$ nuclei by neutron capture is sensitive to the neutron capture cross section of $^{130}$Sn. This sensitivity arises as a consequence of the long $\beta$-decay lifetime of $^{130}$Sn, $\tau_\beta = 162$ s, which allows only relatively small amounts of material to exit $^{130}$Sn by $\beta$-decay. These factors cause significant amounts of material to be directed primarily along the neutron capture channel of

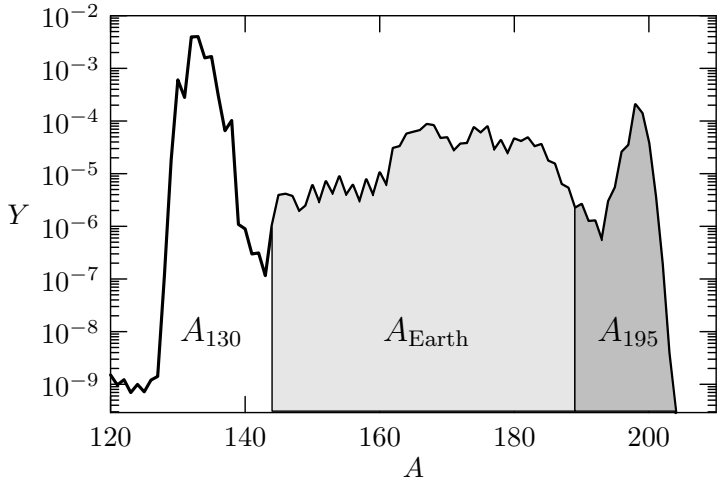


**Figure 2.** We show the $r$-process abundance pattern in the neutrino-driven wind for an entropy per baryon of $s/k = 100$, an outflow timescale of $\tau = 0.3$ s, and an initial electron fraction of $Y_e = 0.26$ at $T_9 = 10$. The shaded areas depict the various peak regions of the $r$-process. The left region (white) shows the second $r$-process peak, the middle region (light gray) shows the rare earth peak region, and the right region (dark gray) shows the third $r$-process peak region.

$^{130}$Sn, and we demonstrate both the flow of material into $^{130}$Sn by $\beta$-decay and the flow of material out of $^{130}$Sn by neutron capture in figure 3.

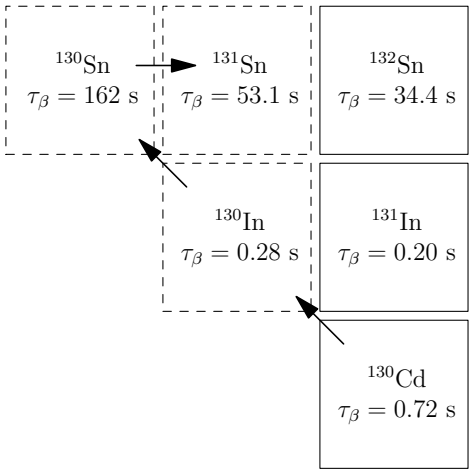


**Figure 3.** We depict the flow of material near $^{130}$Sn. Rightward arrows indicate the direction of the neutron capture reaction channel, and the arrows that point along the diagonal indicate the direction of $\beta$-decay. A significant amount of material arrives at $^{130}$Sn from the $\beta$-decay of the $A = 130$ path nucleus $^{130}$Cd. Depending on the neutron capture cross section of $^{130}$Sn, some fraction of this material is re-directed along the $Z = 50$ neutron capture reaction channel. The conditions here are the same as in figure 2.

We now examine how the uncertainties in the neutron capture cross section of $^{130}$Sn

affect the neutron capture reaction channel of $^{130}$Sn and the consequences that these uncertainties present to the $r$-process. Although the neutron capture cross section of $^{130}$Sn is fairly consistent between the theoretical models that are depicted in figure 1, our understanding of the cross section is not complete. For example, Rauscher et al. 1997 examined the direct-capture portion of the capture cross section of neutrons on nuclei and found that the direct-capture cross section varies by several orders of magnitude between the different theoretical models for $^{130}$Sn [46]. In order to probe the influence of the uncertainties in the cross section, we introduce a scaling factor, $\chi$, which modifies the $^{130}$Sn neutron capture cross section

$$\langle v\sigma_{n,\gamma}(^{130}\mathrm{Sn})\rangle' = \chi\langle v\sigma_{n,\gamma}(^{130}\mathrm{Sn})\rangle \tag{1}$$

Above, $\langle v\sigma_{n,\gamma}(^{130}\mathrm{Sn})\rangle$ is the original, thermally averaged, neutron capture cross section of $^{130}$Sn, $\langle v\sigma_{n,\gamma}(^{130}\mathrm{Sn})\rangle'$ is the modified neutron capture cross section of $^{130}$Sn, and $\chi$ is a scalar multiplication factor. Changes to the neutron capture cross section of $^{130}$Sn induce a corresponding change in the photo-dissociation rate, $\lambda_\gamma$, of $^{131}$Sn,

$$\lambda'_\gamma(^{131}\mathrm{Sn}) = \chi\lambda_\gamma(^{131}\mathrm{Sn}) \tag{2}$$

Above, $\lambda_\gamma(^{131}\mathrm{Sn})$ is the original photo-dissociation rate of $^{131}$Sn and $\lambda'_\gamma(^{131}\mathrm{Sn})$ is the modified photo-dissociation rate of $^{131}$Sn.

We examine the $r$-process in the neutrino driven wind for increases to the neutron capture cross section by a factor of 10 and 100 ($\chi$ = 10, 100). For these cases the photo-dissociation rate of $^{131}$Sn is also increased by a factor of 10 and 100 respectively. We take the $r$-process that forms in the neutrino-driven wind under the conditions that are described in section 2 as our baseline for comparison.

Under an increase in the neutron capture cross section of $^{130}$Sn, changes in the $r$-process abundance pattern relative to the baseline occur not only for nuclei near $^{130}$Sn, but also throughout the $r$-process abundance pattern. Changes to the abundance near $^{130}$Sn due to an increase in the neutron capture cross section of $^{130}$Sn by a factor of 100 include a decrease in the abundance of the $A = 130$ nuclei by $\sim 93\%$ and an increase in the abundance of the $A = 131$ nuclei by $\sim 191\%$. Global effects to the abundance pattern include changes to the abundance of individual nuclear species above the second $r$-process peak region by as much as $\sim 34\%$. The average percent change in abundance for this increase in the cross section is $\sim 12\%$. Although the percent change in abundance is less when the neutron capture cross section of $^{130}$Sn is increased by a factor of 10, global changes to the abundance pattern still occur. The impact an increase in the neutron capture cross section of $^{130}$Sn has on the $r$-process abundance pattern is shown in figure 4.

An increase of the $^{130}$Sn neutron capture cross section acts to hasten both the depletion of $^{130}$Sn and the production of $^{131}$Sn. This is depicted in figure 5(a). A surprising consequence that results from increasing the cross section of $^{130}$Sn is that enough neutrons are consumed in the production of $^{131}$Sn by the neutron capture on $^{130}$Sn to significantly influence the availability of neutrons for capture by other $r$-process

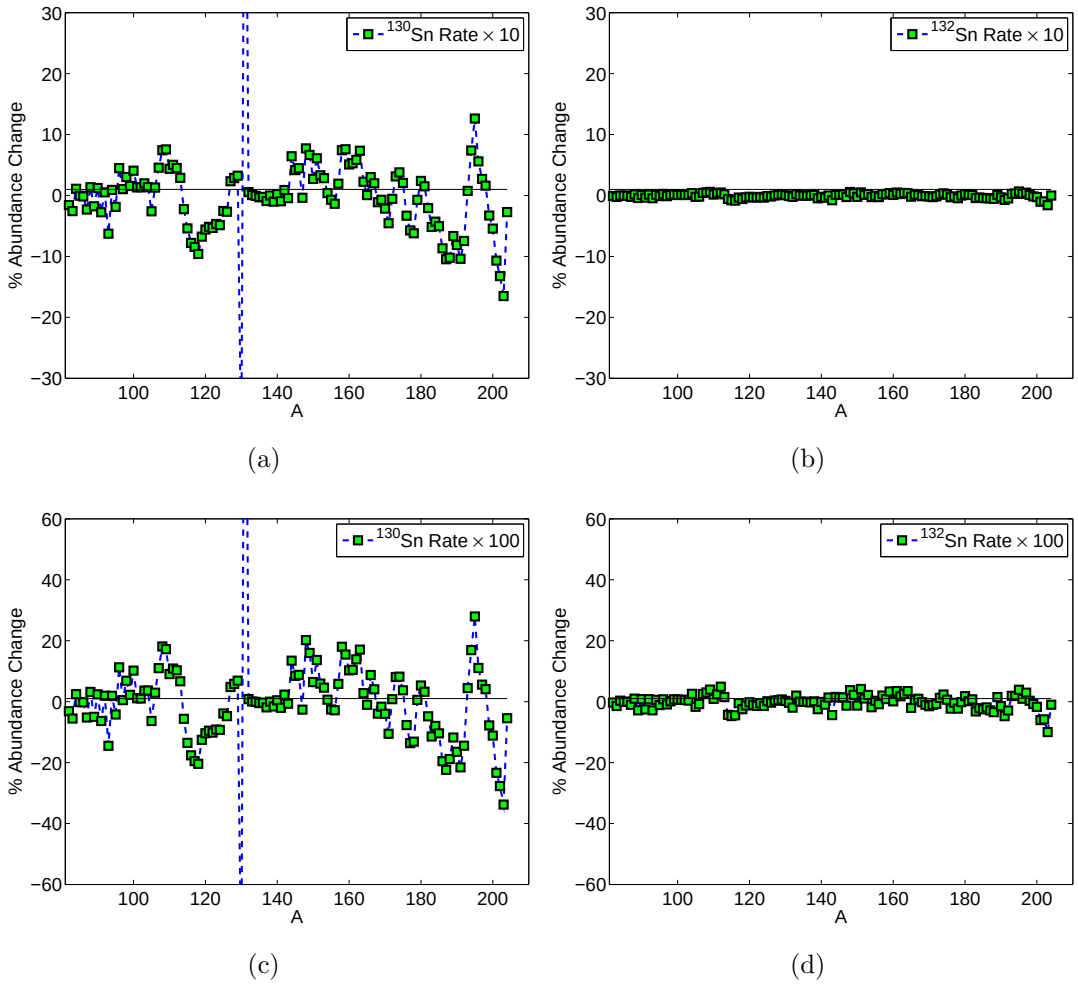


**Figure 4.** The percent change in abundance for an $r$-process calculation under an increase in the neutron capture cross section of $^{130}$Sn with respect to the baseline calculation is shown. The top left panel depicts the percent change when the neutron capture cross section of $^{130}$Sn is increased by a factor of 10, and the bottom left panel depicts the percent change for an increase by a factor of 100. This is contrasted with the percent change in abundance due to changing the neutron capture cross section of $^{132}$Sn by a factor of 10, top right panel, and by a factor of 100, bottom right panel.

nuclei. This effect can be quantified by the net rate of neutron capture,

$$\dot{\eta}(Z,A) = n_n\langle v\sigma_{n,\gamma}(Z,A)\rangle Y(Z,A) - \lambda_\gamma(Z,A+1)Y(Z,A+1) \tag{3}$$

The net rate of neutron capture is the instantaneous rate of neutrons that are captured or released in $(n,\gamma)$ reactions between the nuclei $(Z,A)$ and $(Z,A+1)$. The increase in the net rate of neutron capture for the second peak region is consequentially balanced by an equivalent decrease in the net rate of neutron capture for the rare earth and third peak regions. This is shown in figure 5(b), where we sum the net rate of neutron capture over each of the $r$-process peak regions, $\sum\dot{\eta}$. The individual $r$-process peak regions are the same as those depicted in figure 2; the $A = 130$ peak region is taken to include

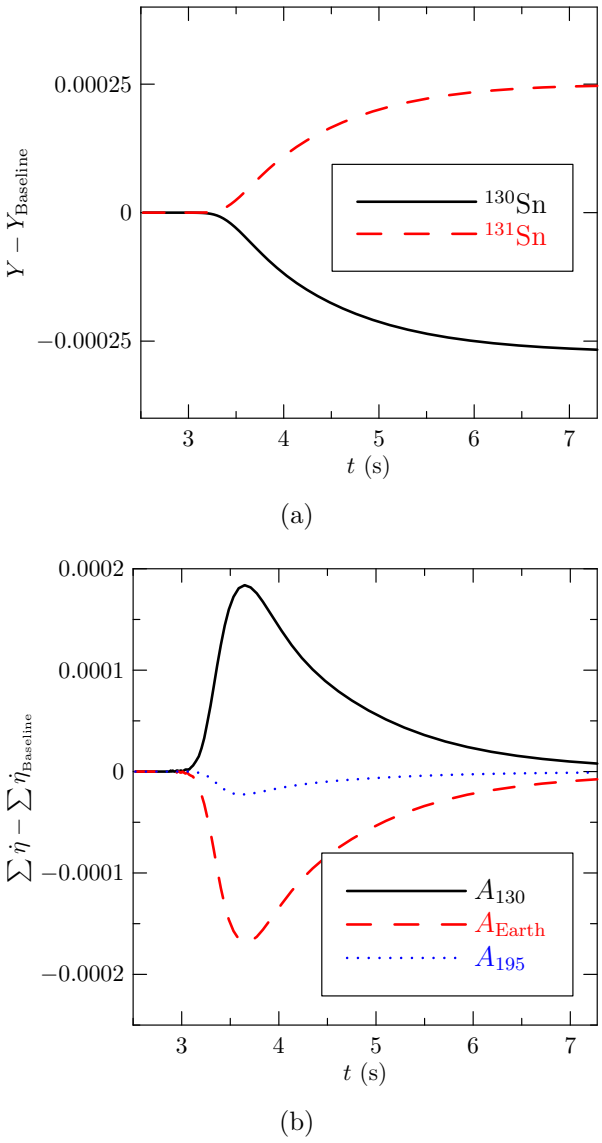


**Figure 5.** In the bottom panel, we show the relative rate of net neutron capture, $\dot{\eta}$, summed over each of the three peak regions of the $r$-process. The absolute difference between an $r$-process with the neutron capture cross section of $^{130}$Sn increased by a factor of 100, $\sum\dot{\eta}$, and that of the baseline calculation, $\sum\dot{\eta}_{\rm Baseline}$, is shown. The increase in the neutron capture cross section of $^{130}$Sn enhances the amount of neutron capture that occurs in the $A \sim 130$ peak and reduces the amount of neutron capture for nuclei in the rare earth and $A \sim 195$ peak regions. In the top panel, we show the absolute difference in the abundance of $^{130}$Sn (solid line) and $^{131}$Sn (dashed line) for an $r$-process with the neutron capture cross section of $^{130}$Sn increased by a factor of 100, $Y$, and the baseline $r$-process calculation with the unaltered set of neutron capture rates, $Y_{\rm Baseline}$. The depicted abundance change in the top panel is commensurate with that expected from increasing the $^{130}$Sn neutron capture rate.

nuclei with $A < 145$, the rare earth peak region includes nuclei between $145 \leq A < 190$, and the $A = 195$ peak region includes nuclei with $A \geq 190$

This reduction in the overall rate of neutron capture above the $A \approx 130$ $r$-process

peak influences the distribution of material within the rare earth and third peak regions by shifting material within these regions towards lighter nuclei in $A$. For an $r$-process under the increased neutron capture cross section, less material reaches the right hand side of the third $r$-process peak, in nuclei with $A \geq 199$, compared with the abundance pattern of the baseline calculation. Additionally, an increase in the abundance of the nuclei is found on the left hand side of the third $r$-process peak in the nuclei between $195 \leq A \leq 198$. A similar effect occurs in the rare earth region of the $r$-process, less material populates the heavier, right hand side of the rare earth region, leading to an increase in the abundance of lighter nuclei within the rare earth region. The impact of the shifting of material in the $r$-process under an increased neutron capture cross section of $^{130}$Sn is depicted in figure 4.

### *3.1. Comparison with $^{132}$Sn (n,γ)*

We contrast our findings for $^{130}$Sn with a classical waiting point nucleus, $^{132}$Sn, which is also being studied at HRIBF [37]. This nucleus, $^{132}$Sn, is both significantly populated at late times in the $r$-process and has a relatively long $\beta$-decay lifetime, similar to $^{130}$Sn. The dynamics of the material flows near $^{132}$Sn depart from that of $^{130}$Sn in a significant way, however. The $(n, \gamma) \rightleftharpoons (\gamma, n)$ counterpart nucleus of $^{132}$Sn, $^{133}$Sn, has a faster photo-dissociation rate than that of $^{131}$Sn, the $(n, \gamma) \rightleftharpoons (\gamma, n)$ counterpart to $^{130}$Sn. This occurs despite the lower neutron capture rate of $^{132}$Sn relative to $^{130}$Sn and is largely due to the smaller neutron separation energy of $^{133}$Sn ($S_n \approx 2.6$ MeV) relative to that of $^{131}$Sn ($S_n \approx 5.1$ MeV). This increased rate of photo-dissociation results in $^{132}$Sn remaining in $(n, \gamma) \rightleftharpoons (\gamma, n)$ equilibrium until very late times in the $r$-process, which in this model corresponds to $t \approx 4.5$ s. After $^{132}$Sn leaves $(n, \gamma) \rightleftharpoons (\gamma, n)$ equilibrium, the $r$-process does gain slight sensitivity to its neutron capture cross section, see figure 4. The free neutron abundance is low as this happens late in the $r$-process, leading to a smaller overall effect to the $r$-process than that for the case of $^{130}$Sn.

## 4. Conclusions

We have shown how the neutron capture cross section of a single nucleus, $^{130}$Sn, can influence the shape the global $r$-process abundance pattern. Changes to the neutron capture cross section of $^{130}$Sn can influence the abundance pattern at late times, shifting material towards lighter nuclei in the rare earth and third peak regions for increases in the neutron capture cross section of $^{130}$Sn. This arises as an increase in the cross section enhances the amount of neutron capture by $^{130}$Sn and reduces the amount of neutron capture in the rare earth and third peak regions. For an increase in the neutron capture cross section of $^{130}$Sn by a factor of 100, we find changes to the abundance of nuclei near $^{130}$Sn are as much as $\sim 191\%$, and changes to the abundance of nuclei near the third peak region are as much as $\sim 34\%$. We find the average percent change in the abundance of the $r$-process nuclei to be $\sim 12\%$. Although smaller increases to the cross

section reduce the size of these effects, we show that an increase in the neutron capture cross section of $^{130}$Sn by a factor of 10 results in similar global changes to the $r$-process abundance pattern. These changes are specific to the astrophysical conditions of the $r$-process and depend on the underlying nuclear data and choice of the thermodynamic model. While the $(n,\gamma) \rightleftharpoons (\gamma,n)$ equilibrium epoch of the $r$-process sets the major features of the abundance pattern of the $r$-process, the details of the physics of the $r$-process freeze-out epoch, including the neutron capture cross section of key nuclei such as $^{130}$Sn, impacts the abundance pattern as well. Experimental investigations of the neutron capture cross section of $^{130}$Sn will help to reduce the uncertainties in this cross section, and the initial efforts are underway at the Hollifield Radioactive Ion Beam Facility (HRIBF).

The influence of the neutron capture reaction for $^{130}$Sn demonstrated in this analysis results from the confluence of three factors; a prominent place on the $r$-process path, a long $\beta$-decay half-life, and a large $Q$ value for the neutron capture. The first two result in a significant abundance of $^{130}$Sn at late times in the $r$-process, while the last causes this reaction to drop out of $(n,\gamma) \rightleftharpoons (\gamma,n)$ equilibrium early enough that significant numbers of neutron captures can occur out of equilibrium. While the half-life and $Q$-value are universal, the dependence on the $r$-process path means that the influence demonstrated here for $^{130}$Sn may not hold for all $r$-process scenarios. However, it is likely that other reactions, with similar characteristics, would have similar influence for these differing scenarios. Determination of the existence and identity of these influential reactions, as well as theoretical and experimental study of their rates, is important to refining our knowledge of the $r$-process.

## Acknowledgments

This work was partially supported by the Joint Institute for Heavy Ion Research at ORNL, the Department of Energy under contracts DE-FG05-05ER41398 (RS), DE FG02-02ER41216 (GCM), and by the National Science Foundation under contract PHY-0244783 (WRH). Oak Ridge National Laboratory is managed by UT-Battelle, LLC, for the U.S. Department of Energy under contract DE-AC05-000R22725.

## 5. References

[1] E. M. Burbidge, G. R. Burbidge, W. A. Fowler, and F. Hoyle. Synthesis of the Elements in Stars. *Reviews of Modern Physics*, 29:547–650, 1957.

[2] A. G. W. Cameron. *Chalk River Rep.*, CRL-41, 1957.

[3] J. J. Cowan, F.-K. Thielemann, and J. W. Truran. The R-process and nucleochronology. *Phys. Rep.*, 208:267–394, November 1991.

[4] J. M. Pearson and S. Goriely. Nuclear mass formulas for astrophysics. *Nuclear Physics A*, 777:623–644, October 2006.

[5] P. Möller, J. R. Nix, W. D. Myers, and W. J. Swiatecki. Nuclear Ground-State Masses and Deformations. *Atomic Data and Nuclear Data Tables*, 59:185–+, 1995.

[6] Y. Aboussir, J. M. Pearson, A. K. Dutta, and F. Tondeur. Nuclear Mass Formula via an Approximation to the Hartree-Fock Method. *Atomic Data and Nuclear Data Tables*, 61:127–+, 1995.

[7] S. E. Woosley and R. D. Hoffman. The alpha-process and the r-process. *ApJ*, 395:202–239, August 1992.

[8] B. S. Meyer, G. J. Mathews, W. M. Howard, S. E. Woosley, and R. D. Hoffman. R-process nucleosynthesis in the high-entropy supernova bubble. *ApJ*, 399:656–664, November 1992.

[9] S. E. Woosley, J. R. Wilson, G. J. Mathews, R. D. Hoffman, and B. S. Meyer. The r-process and neutrino-heated supernova ejecta. *ApJ*, 433:229–246, September 1994.

[10] K. Takahashi, J. Witti, and H.-T. Janka. Nucleosynthesis in neutrino-driven winds from protoneutron stars II. The r-process. *A&A*, 286:857–869, June 1994.

[11] Y.-Z. Qian and S. E. Woosley. Nucleosynthesis in Neutrino-driven Winds. I. The Physical Conditions. *ApJ*, 471:331–+, November 1996.

[12] C. Y. Cardall and G. M. Fuller. General Relativistic Effects in the Neutrino-driven Wind and r-Process Nucleosynthesis. *ApJ*, 486:L111+, September 1997.

[13] K. Otsuki, H. Tagoshi, T. Kajino, and S.-y. Wanajo. General Relativistic Effects on Neutrino-driven Winds from Young, Hot Neutron Stars and r-Process Nucleosynthesis. *ApJ*, 533:424–439, April 2000.

[14] K. Sumiyoshi, H. Suzuki, K. Otsuki, M. Terasawa, and S. Yamada. Hydrodynamical Study of Neutrino-Driven Wind as an r-Process Site. *PASJ*, 52:601–611, August 2000.

[15] S. Wanajo, T. Kajino, G. J. Mathews, and K. Otsuki. The r-Process in Neutrino-driven Winds from Nascent, "Compact" Neutron Stars of Core-Collapse Supernovae. *ApJ*, 554:578–586, June 2001.

[16] T. A. Thompson, A. Burrows, and B. S. Meyer. The Physics of Proto-Neutron Star Winds: Implications for r-Process Nucleosynthesis. *ApJ*, 562:887–908, December 2001.

[17] I. V. Panov and H. . Janka. On the Dynamics of Proto-Neutron Star Winds and r-Process Nucleosynthesis. *ArXiv e-prints*, 805, May 2008.

[18] K. Sumiyoshi, M. Terasawa, G. J. Mathews, T. Kajino, S. Yamada, and H. Suzuki. r-Process in Prompt Supernova Explosions Revisited. *ApJ*, 562:880–886, December 2001.

[19] S. Wanajo, M. Tamamura, N. Itoh, K. Nomoto, Y. Ishimaru, T. C. Beers, and S. Nozawa. The r-Process in Supernova Explosions from the Collapse of O-Ne-Mg Cores. *ApJ*, 593:968–979, August 2003.

[20] C. Freiburghaus, S. Rosswog, and F.-K. Thielemann. R-Process in Neutron Star Mergers. *ApJ*, 525:L121–L124, November 1999.

[21] S. Goriely, P. Demetriou, H.-T. Janka, J. M. Pearson, and M. Samyn. The r-process nucleosynthesis: a continued challenge for nuclear physics and astrophysics. *Nuclear Physics A*, 758:587–594, July 2005.

[22] R. Surman, G. C. McLaughlin, M. Ruffert, H. Th. Janka, and W. R. Hix. r-Process Nucleosynthesis in Hot Accretion Disk Flows from Black Hole - Neutron Star Mergers. 2008.

[23] R. Surman and G. C. McLaughlin. Neutrinos and Nucleosynthesis in Gamma-Ray Burst Accretion Disks. *ApJ*, 603:611–623, March 2004.

[24] R. Surman, G. C. McLaughlin, and W. R. Hix. Nucleosynthesis in the outflow from gamma ray burst accretion disks. *Astrophys. J.*, 643:1057–1064, 2006.

[25] G. C. McLaughlin and R. Surman. Prospects for obtaining an r process from Gamma Ray Burst Disk Winds. *Nuclear Physics A*, 758:189–196, July 2005.

[26] A. I. MacFadyen and S. E. Woosley. Collapsars: Gamma-Ray Bursts and Explosions in "Failed Supernovae". *ApJ*, 524:262–289, October 1999.

[27] J. Pruet, T. A. Thompson, and R. D. Hoffman. Nucleosynthesis in Outflows from the Inner Regions of Collapsars. *ApJ*, 606:1006–1018, May 2004.

[28] H. Ning, Y. Z. Qian, and B. S. Meyer. r-process nucleosynthesis in shocked surface layers of o-ne-mg cores. 2007.

[29] H. Th. Janka, B. Mueller, F. S. Kitaura, and R. Buras. Dynamics of shock propagation and nucleosynthesis conditions in o-ne-mg core supernovae. 2007.

[30] R. Surman and J. Engel. Changes in r-process abundances at late times. *Phys. Rev. C*, 64(3):035801, Aug 2001.

[31] T. Rauscher. Neutron capture in the r-process – do we know them and does it make any difference? *Nuclear Physics A*, 758:655, 2005.

[32] K. Farouqi, K.-L. Kratz, B. Pfeiffer, T. Rauscher, and F.-K. Thielemann. Neutron captures and the r-process. In A. Woehr and A. Aprahamian, editors, *Capture Gamma-Ray Spectroscopy and Related Topics*, volume 819 of *American Institute of Physics Conference Series*, pages 419–422, March 2006.

[33] S. Goriely. Radiative neutron captures by neutron-rich nuclei and the r-process nucleosynthesis. *Physics Letters B*, 436:10–18, September 1998.

[34] S. Goriely. Direct neutron captures and the r-process nucleosynthesis. *A&A*, 325:414–424, September 1997.

[35] T. Rauscher. Neutron Captures and the r-Process. In Y.-Z. Qian, E. Rehm, and H. Schatz, editors, *The r-Process: The Astrophysical Origin of the Heavy Elements and Related Rare Isotope Accelerator Physics*, pages 63–+, 2004.

[36] R. L. Kozub, J. F. Shriner, Jr., A. Adekola, D. W. Bardayan, J. C. Blackmon, F. Liang, C. D. Nesaraja, D. Shapira, M. S. Smith, K. Y. Chae, K. L. Jones, Z. Ma, B. H. Moazen, K. Chipps, L. Erikson, J. A. Cizewski, R. Hatarik, S. D. Pain, C. Matei, W. Krolas, and T. P. Swan. Single particle states in ˆ131Sn and the r-process. *APS Meeting Abstracts*, pages H10+, October 2007.

[37] K. Jones. The single-particle structure around ˆ132Sn explored through the (d,p) reaction. *APS Meeting Abstracts*, pages 2002–+, April 2007.

[38] J. Beun, G. C. McLaughlin, R. Surman, and W. R. Hix. Fission cycling in supernova nucleosynthesis: Active-sterile neutrino oscillations. *Phys. Rev. D*, 73(9):093007–+, May 2006.

[39] J. Beun, G. C. McLaughlin, R. Surman, and W. R. Hix. Fission cycling in a supernova r process. *Phys. Rev. C*, 77(3):035804–+, March 2008.

[40] W. R. Hix and F. K. Thielemann. Computational methods for nucleosynthesis and nuclear energy generation. *J. Comp. App. Math.*, 109:321–+, 1999.

[41] T. Rauscher and F.-K. Thielemann. Astrophysical Reaction Rates From Statistical Model Calculations. *Atomic Data and Nuclear Data Tables*, 75:1–2, May 2000.

[42] R. Surman and J. Engel. Changes in r-process abundances at late times. *Phys. Rev. C*, 64(3):035801–+, September 2001.

[43] R. Surman, J. Engel, J. R. Bennett, and B. S. Meyer. Source of the Rare-Earth Element Peak in r-Process Nucleosynthesis. *Physical Review Letters*, 79:1809–1812, September 1997.

[44] P. Möller and J. Randrup. New developments in the calculation of $\beta$-strength functions. *Nuclear Physics A*, 514:1–48, July 1990.

[45] P. Möller, B. Pfeiffer, and K.-L. Kratz. New calculations of gross $\beta$-decay properties for astrophysical applications: Speeding-up the classical r process. *Phys. Rev. C*, 67(5):055802–+, May 2003.

[46] T. Rauscher, K.-L. Kratz, H. Oberhummer, J. Dobaczewski, P. Moeller, and M. Sharma. Uncertainties in direct neutron capture calculations due to nuclear structure models. *Nuclear Physics A*, 621:327–330, August 1997.